Sr_2RuO_4: A metallic substrate for the epitaxial growth of $YBa_2Cu_3O_{7-\delta}$

F. Lichtenberg, A. Catana, J. Mannhart, and D. G. Schlom
IBM Research Division, Zurich Research Laboratory, 8803 Rüschlikon, Switzerland

(Received 7 November 1991; accepted for publication 10 December 1991)

Single crystals of Sr_2RuO_4 were grown by the floating zone melting technique. The crystals have the K_2NiF_4 structure and display a metallic resistivity behavior in the *a-b*-plane between 300 and 4.2 K ($\rho_{ab} \simeq 10^{-4}$ Ω cm at 300 K). The in-plane lattice mismatch between $YBa_2Cu_3O_{7-\delta}$ (001) and Sr_2RuO_4 (001) is smaller than 1.3%, better than that to $SrTiO_3$ {100}. Epitaxial films of $YBa_2Cu_3O_{7-\delta}$ with $T_c(R=0)$ as high as 86 K have been grown on Sr_2RuO_4 crystals. The epitaxial growth of $YBa_2Cu_3O_{7-\delta}$ on Sr_2RuO_4 was revealed by 4-circle x-ray diffraction as well as by transmission electron microscopy.

For many device applications of high-T_c superconductors it is desirable to employ metals that are compatible with high-T_c materials. Such metals may be used in thin-film form for SNS heterostructures (S = superconductor, N = normal metal) or as substrates with high thermal conductivity. Searching for such materials, we have grown single crystals of Sr_2RuO_4, which is a paramagnetic conductor with the K_2NiF_4 structure[1,2] and an excellent lattice match to $YBa_2Cu_3O_{7-\delta}$ (at 300 K, Sr_2RuO_4 is tetragonal with $a = 3.87$ Å and $YBa_2Cu_3O_{7-\delta}$ is orthorhombic with $a = 3.82$ Å and $b = 3.89$ Å). This lattice mismatch compares favorably to that between $YBa_2Cu_3O_{7-\delta}$ (001) and $SrTiO_3$ {100} (cubic with $a = 3.91$ Å at 300 K). $SrTiO_3$ is a standard insulating substrate for the growth of superconducting copper oxides. Thin films of $YBa_2Cu_3O_{7-\delta}$ were deposited onto the *a-b*-plane of Sr_2RuO_4 by hollow cathode magnetron sputtering. In the following, we describe the preparation of Sr_2RuO_4 crystals, their electrical characteristics, and those of epitaxial $YBa_2Cu_3O_{7-\delta}$ films on Sr_2RuO_4.

To fabricate the Sr_2RuO_4 crystals, appropriate molar ratios of $SrCO_3$ (JMC, puratronic) and RuO_2 (Alfa Products, 99.9%) were weighed with an accuracy of 1 mg to a total weight of several grams. After grinding, the powder was mixed with water and pressed into two rods of 5-mm diameter each, one of which is 10-mm and the other 100-mm long. The rods were sintered on Al_2O_3 boats in air at 1300 °C. Using the floating zone process, the ceramic rods were melted in air in an elliptical mirror cavity with focused infrared radiation. The short rod was used as the seed and the long rod as the feed material. The melt-grown samples were cylindrical in shape and the layers (*a-b*-planes) of Sr_2RuO_4 were found to grow along the axis of the cylinder.

The growth of Sr_2RuO_4 crystals is complicated by the volatility of RuO_2, which leads to the segregation of SrO. To compensate for this loss, an excess of RuO_2 was used in the starting material, e.g., a molar ratio of 2:1.1 between $SrCO_3$ and RuO_2. Despite this compensation, the surface of melt-grown cylinders was polycrystalline and contained SrO, as shown by x-ray powder diffraction.

In order to grow large crystals, it is necessary to keep the amount of molten material nearly constant; however, the melt volume frequently shrank during growth. This was probably due to both the low density of the sintered rods and the continuous evaporation of RuO_2. The latter resulted in a layer of RuO_2 being deposited on the interior of the silica tube of the floating zone melting furnace. This layer diminishes the infrared transmission of the silica tube. To maintain a constant melt volume, the infrared power was continually increased, making it possible to grow a Sr_2RuO_4 cylinder with a length of about 10 mm and a diameter of about 5 mm. Owing to the layered nature of Sr_2RuO_4, such a cylinder can easily be cleaved, yielding several highly oriented crystals with (001) surfaces (as determined by Laue diffraction) and surface areas of about 20 mm.[2]

Bulk structural analysis was carried out by x-ray powder diffraction (SIEMENS Diffractometer D 500) with Cu $K\alpha$ radiation. Table I shows the x-ray powder diffraction data of Sr_2RuO_4 at room temperature. All observed peaks (see Table I) fit a body-centered tetragonal unit cell of the K_2NiF_4 type with lattice constants $a = b = 3.87$ Å and $c = 12.74$ Å, which is in agreement with earlier results from polycrystalline material.[1,2]

Resistivity measurements of small Sr_2RuO_4 crystals cleaved from the melt-grown samples were performed between room temperature and 4.2 K using a four-point geometry. Electrical contacts were made by indium dots or silver paint. After the resistivity was measured along the *c*-axis of Sr_2RuO_4, performed by attaching one voltage and one current electrode to either (001) face of the crystal, the contacts were then removed and new contacts were made for the resisitivity measurements in the *a-b*-plane.

Figure 1 shows the resistivity versus temperature of a small crystal of Sr_2RuO_4. To check the temperature dependence of the resistivity, several crystals of different geometries were measured. The raw data shown in Fig. 1 are from a crystal with the dimensions $2 \times 1 \times 0.1$ mm, and are representative of the behavior of all samples measured. For ρ_c no corrections for inhomogeneous current density distribution were made. However, the absolute values of the resistances as well as measurements on samples with other contact geometries indicate that the temperature dependence of the uncorrected resistivity ρ_c is that of the true resistivity.

In the *a-b*-plane the resistivity ranges from $\rho_{ab} \simeq 10^{-4}$ Ω cm at room temperature down to $\rho_{ab} \simeq 10^{-6}$ Ω cm at 4.2 K, demonstrating the highly conductive metallic in-plane behavior of Sr_2RuO_4. The resistivity observed along the

 0003-6951/92/091138-03$03.00

TABLE I. Observed x-ray powder diffraction data (index "obs") of Sr_2RuO_4 and calculated values (index "calc") on the basis of a body-centered tetragonal unit cell.

n	$h\,k\,l$	d_{calc}[Å]	d_{obs}(Å)	I_{obs}
1	0 0 2	6.3711	6.3766	30
2	1 0 1	3.7032	3.7035	2
3	0 0 4	3.1855	3.1845	1
4	1 0 3	2.8607	2.8592	100
5	1 1 0	2.7367	2.7361	58
6	1 1 2	2.5145		
7	1 0 5	2.1284		
8	0 0 6	2.1237	2.1239	47
9	1 1 4	2.0758	2.0752	6
10	2 0 0	1.9351	1.9348	27
11	2 0 2	1.8516	1.8523	2
12	2 1 1	1.7151		
13	1 1 6	1.6778	1.6778	18
14	2 0 4	1.6539		
15	1 0 7	1.6472		
16	2 1 3	1.6029	1.6029	22
17	0 0 8	1.5928	1.5928	6
18	2 1 5	1.4318		
19	2 0 6	1.4304	1.4304	17
20	1 1 8	1.3766	1.3765	6
21	2 2 0	1.3684	1.3684	3
22	2 2 2	1.3378		
23	1 0 9	1.3296	1.3297	5

c-axis resembles that of the layered materials TaS_2 and graphite. Like Sr_2RuO_4, they exhibit a metallic behavior along the layers and a resisitivity maximum between room temperature and 4.2 K perpendicular to the layers.[3–5]

$YBa_2Cu_3O_{7-\delta}$ films were deposited by hollow cathode magnetron sputtering[6] on the (001) surface of the Sr_2RuO_4 crystals. The freshly cleaved substrates were attached to the heater of the sputtering chamber with silver paint. The sputter parameters used were a substrate heater block temperature of 740–750 °C, a total pressure ($Ar/O_2 = 2{:}1$) of 650 mTorr, a plasma discharge of 150–170 V and 450 mA, and an aftergrowth cool-down in $\simeq 0.5$ bar O_2 lasting $\simeq 1$ h.

Four-point resistance measurements performed on such films indicated good superconducting properties. Figure 2 shows the best temperature dependence of the resistance achieved so far: zero resistivity at 86 K and a transition width of about 1 K for a 120-nm-thick film. The contact resistance between the $YBa_2Cu_3O_{7-\delta}$ film and the Sr_2RuO_4 substrate (of the same sample shown in Fig. 2) was measured to be $< 10^{-6}\ \Omega\ cm^2$.

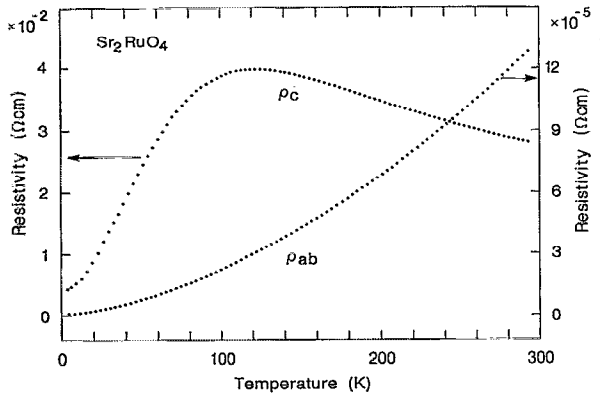

FIG. 1. Resistivity vs temperature of Sr_2RuO_4 in the a-b-plane (indicated by ρ_{ab}) and along the c-axis (indicated by ρ_c). See text for discussion of ρ_c.

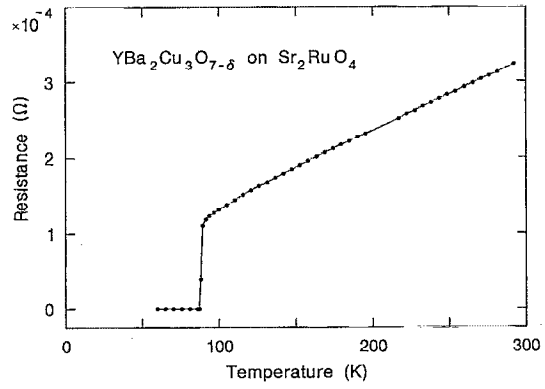

FIG. 2. Resistance vs temperature of a $YBa_2Cu_3O_{7-\delta}$ film grown on the (001) surface of Sr_2RuO_4.

The epitaxial relationship between a $YBa_2Cu_3O_{7-\delta}$ film and a Sr_2RuO_4 substrate was investigated by x-ray diffraction using a 4-circle diffractometer in the Bragg-Brentano geometry with CuK_α radiation. These x-ray diffraction measurements revealed that $YBa_2Cu_3O_{7-\delta}$ grows epitaxially on Sr_2RuO_4 with $YBa_2Cu_3O_{7-\delta}(001)\|Sr_2RuO_4(001)$ and $YBa_2Cu_3O_{7-\delta}[100]\|Sr_2RuO_4\langle 100\rangle$. A θ-2θ x-ray scan aligned to the Sr_2RuO_4 (001) substrate is shown in Fig. 3(a). The scan demonstrates that the $YBa_2Cu_3O_{7-\delta}$ films is oriented with its c-axis normal to the plane of the substrate. The in-plane alignment of the film and substrate axes was determined by pole figure type x-ray diffraction scans in which the sample was positioned to diffract from an inclined film plane and was subsequently rotated about an axis normal to the substrate plane (a ϕ-scan). The ϕ-scan of the 103 reflection of $YBa_2Cu_3O_{7-\delta}$ is shown in Fig. 3(b). The four peaks (every 90°) indicate that the $YBa_2Cu_3O_{7-\delta}$ has grown epitaxially on the Sr_2RuO_4 substrate with in-plane alignment of the perovskite axes of the film and substrate. Note that the 103 $YBa_2Cu_3O_{7-\delta}$ film reflection does not overlap with any hkl reflection of the Sr_2RuO_4 substrate, owing to the distinct c-axis lengths of the two materials.

Additional structural information was obtained by electron diffraction and transmission electron microscopy (TEM) with a JEM-2010 operated at 200 kV. For this purpose, thin specimens were prepared by mechanical grinding and polishing of the substrate and subsequent ion beam thinning ($I = 5$ mA, $V = 4$ kV). Images were recorded under axial illumination conditions, with the electron beam parallel to the substrate normal. In Fig. 4, a TEM lattice image and the corresponding diffraction pattern of a film are shown. The deposition conditions for this sample, not the same as those shown in Fig. 3, were such that both c- and a-b-axis oriented regions were present. In

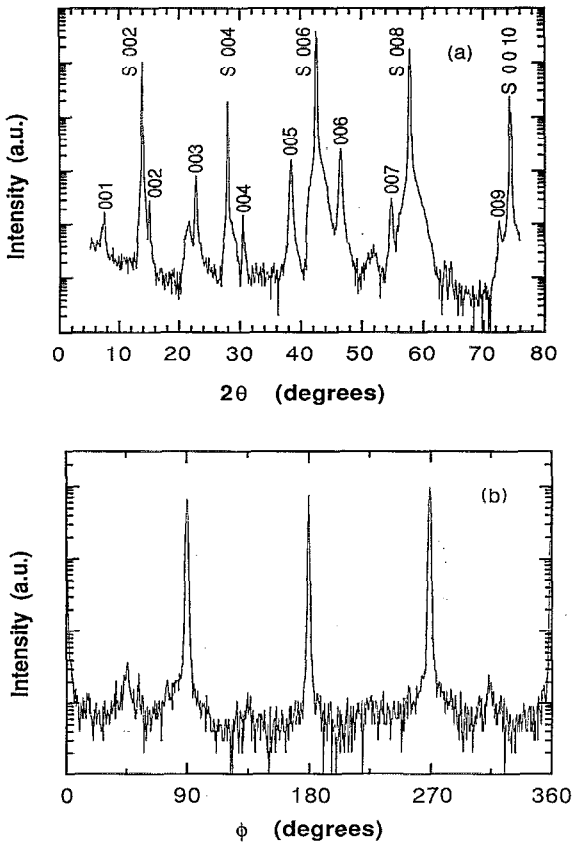

FIG. 3. (a) θ-2θ x-ray diffraction scan aligned to the Sr_2RuO_4(001) substrate plane. The label S denotes substrate peaks. (b) ϕ x-ray diffraction scan of the 103 reflection of $YBa_2Cu_3O_{7-\delta}$. $\phi \equiv 0$ is set parallel to the Sr_2RuO_4[100] axis. The c-axis lattice spacing of $YBa_2Cu_3O_{7-\delta}$ calculated from the data in (a) is $c = 11.72 \pm 0.03$ Å.

addition to the characteristic $YBa_2Cu_3O_{7-\delta}$ film reflections, the diffraction pattern shows spots close to one half of the 110 reflection positions of $YBa_2Cu_3O_{7-\delta}$ which are believed to be due to Y_2O_3 precipitates.[7]

Large crystals of Sr_2RuO_4 have proved difficult to prepare. Methods other than the floating zone melting technique are needed to prepare Sr_2RuO_4 substrates in a more viable manner. However, Sr_2RuO_4 can likely be grown by standard thin-film techniques on commonly used substrates such as $SrTiO_3$. Further studies, such as critical current and surface resistance measurements as well as investigations of $Sr_2RuO_4/YBa_2Cu_3O_{7-\delta}$ diffusion couples,

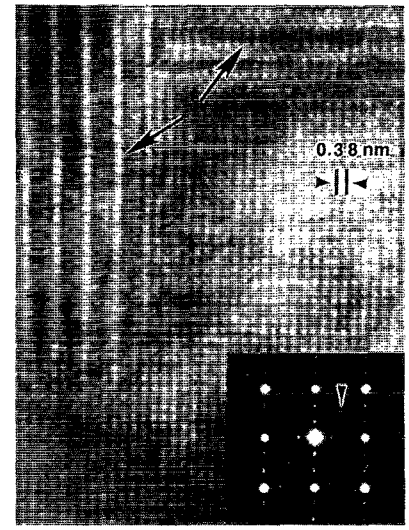

FIG. 4. Plan-view TEM lattice image of an epitaxially grown $YBa_2Cu_3O_{7-\delta}$ film on Sr_2RuO_4. The a-b-axis oriented regions are denoted by arrows. The diffraction pattern (inset) clearly shows that aside from the $YBa_2Cu_3O_{7-\delta}$ reflections, additional spots occur (arrow). They were indexed as Y_2O_3.

will clarify the potential of Sr_2RuO_4 with respect to the field of high-T_c superconductivity.

We wish to thank J. G. Bednorz and K. A. Müller for stimulating interactions. We also gratefully acknowledge J.-P. Locquet and C. Rossel for helpful discussions, G. Rudack, A. Segmüller, and the Laser Science and Technology Department at the IBM Zurich Research Laboratory for their support, and the National Science Foundation Material Research Laboratory at the Center for Materials Research at Stanford University for the use of a 4-circle x-ray diffractometer.

[1] A. Callaghan, C. W. Moeller, and R. Ward, Inorg. Chem. **5**, 1572 (1966).
[2] J. Randall and R. Ward, J. Am. Chem. Soc. **81**, 2629 (1959).
[3] J. A. Wilson, F. J. Di Salvo, and S. Mahajan, Adv. Phys. **24**, 117 (1975).
[4] W. Primak and L. H. Fuchs, Phys. Rev. **95**, 22 (1954).
[5] *Chemistry and Physics of Carbon* (Marcel Dekker, New York, 1973), Vol. 11, pp. 114–115.
[6] J. Geerk, X. X. Xi, H. C. Li, W. Y. Guan, P. Kus, M. Höbel, G. Linker, O. Meyer, F. Ratzel, C. Schultheiss, R. Smithey, B. Strehlau, and F. Weschenfelder, Int. J. Mod. Phys. B **3**, 923 (1989).
[7] A. Catana, R. F. Broom, J. G. Bednorz, J. Mannhart, and D. G. Schlom, Appl. Phys. Lett. **60**, 1016 (1992).